

Multiple Crack Weight for Solution of Multiple Interacting Cracks by Meshless Numerical Methods

Boris Muravin¹, Eli Turkel²

¹ Margan Physical Diagnostics Ltd., Ha-Omanut 12, Netanya, 42160, Israel
Tel: +972-9-8655510, Fax: +972-9-8655514, E-mail: bm@margan.com

² Department of Applied Mathematics, Tel-Aviv University, Tel-Aviv, Israel

Abstract

We devise a multiple crack weight (MCW) method for the accurate and effective solution of strongly interacting cracks by meshless numerical methods. The MCW method constructs weight functions around cracks so that they simultaneously characterize all the cracks present in the single nodal domain of influence. This approach reduces the number of nodes necessary to achieve sufficient accuracy and consequently it decreases the computational effort. Numerical examples demonstrate that the method allows an accurate solution of multiple cracks problems. Convergence of the method is analyzed and discussed.

Keywords: meshless methods, multiple crack weight, multiple interacting cracks.

Introduction

Interaction between multiple cracks is one of the most important but less investigated phenomenon in fracture mechanics. Stress corrosion cracking, hydrogen embrittlement, creep micro-cracking and other common fracture mechanisms are characterized by systems of interacting flaws. Theoretical research of this class of problems is hindered by limitations of the existing numerical methods.

The numerical solution by the traditional finite element method (FEM), of fracture mechanics problems with multiple cracks requires an enormous mesh refinement near each crack tip, including the embedding of many singular elements. Moreover, solution by FEM of dynamic cracks is limited to simple cases. This is because modeling of growing discontinuities requires time consuming remeshing at every time step. For this reason an adaptive FEM has become essential. However adaptive remeshing and mapping of variables is a difficult, computationally expensive task and is a source of cumulative numerical errors. The development of meshless methods [1-9] and the extended finite elements method (X-FEM) [10] in recent years has enabled the solution of problems with growing cracks without remeshing. Nevertheless, these methods continue to be computationally expensive when solving multiple cracks because of the large nodal densities needed in meshless methods and the fine meshes needed in X-FEM for an accurate solution. Therefore, there is a continual effort to improve the accuracy without increasing the degrees of freedom.

We focus on improvements to meshless methods for the solution of fracture mechanics problems. Although X-FEM has recently received greater attention than

meshless methods, they remain an efficient and accurate approach to solve fracture mechanics problems. Recent developments of meshless methods for the solution of different classes of problems such as multiple interacting cracks [11], 3D cracks [12], and cracks in elastic-plastic materials [13] improve these numerical methods, make them more attractive to the user.

There are two main approaches, in meshless methods, for modeling discontinuities and capturing singular stresses at the crack tip. The first one is based on the incorporation of a jump function along the discontinuity and a specific near crack-tip displacement solution in the extrinsic basis [14]. This approach was adopted from X-FEM and has similar limitations. The enrichment area is limited when multiple cracks are densely distributed or when crack tips are close to the boundaries. Modeling of moving cracks in dynamic problems requires the incorporation of different near crack-tip solutions which depends on the crack velocity. In addition, enrichment for developing cracks in elastic-plastic materials is not yet established.

Many of these limitations can be avoided by using another approach which is based on a special modification of the weight functions at the crack tip. For this purpose, several methods have been devised: *the visibility* method [1,15], *the "see-through"* method [16], *the transparency* method [6,17], *the wedge model* [18] and *the diffraction* method [6,17]. The first developed schemes were the *visibility* and *"see-through"* methods. They provide an accurate solution only when very large nodal densities are used. In the visibility method, this is because the weight and shape functions are discontinuous near the crack tip and the size of the discontinuity is a function of the nodal spacing. Although, the "see-through" method provides continuous approximations, it effectively shortens the crack and does not properly capture the singular stress at the crack tip. The transparency method and the wedge model provide more accurate results, however they have a restriction on the position of nodes limiting their use in dynamic crack problems.

Duflot and Nguyen-Dang [19] proposed an *enriched weight function* method. In this method the diffraction weight functions of three nodes near the crack tip are multiplied by the square root of the distance from the crack tip leading to more accurate capture of the singular stresses. However, no analysis of the displacement and the stress field at the crack tip was performed to demonstrate that only three enriched nodes are sufficient to capture the singular stresses and to enforce the zero displacement condition at the crack tip. Nevertheless, calculated stress intensity factors showed greater accuracy using the enriched weight functions compared with an ordinary diffraction approximation. In the current formulation, the enriched nodes are moved together with the crack tip. Hence, the application of this method appears to be limited to static and quasi static cases.

Most recently, *the spiral weight* method [20] for the construction of weight functions around crack tips was developed to increase the accuracy of meshless approximations for the practically important case of a linear basis. This takes into account the advantages and drawbacks of other methods that modify weight function shape around cracks. The spiral weight functions are constructed to preserve the discontinuity along the entire crack length. Numerical examples show that the spiral weight method is more accurate than the diffraction method when using a linear basis.

We design the multiple crack weight method. This method defines the nodal weight functions so that they simultaneously characterize all the cracks and their tips that are present in the domain of influence. This approach reduces the number of nodes necessary for accurate solutions.

Multiple Crack Weight Method

We develop an algorithm for the construction of weight functions to handle multiple interacting cracks, when the distance between cracks can be smaller than the domain of influence of the nodes. This algorithm extends the application of methods that modify the shape of weight functions near a crack to the case of multiple cracks. Among the methods that can be extended for the solution of multiple cracks according to the developed below algorithm are the spiral weight, diffraction, transparency and visibility methods. The algorithm creates a nodal weight function that simultaneously characterizes all the crack tips located in the nodal domain of influence. For simplicity of presentation, the algorithm will be presented for the example of the diffraction method. We call this method the *multiple crack weight* (MCW) method.

Weight functions used in meshless approximations may have different shapes of domain of influence. The most common are the circle and the rectangle. For the circular domain of influence a frequently used weight function is the quadratic spline:

$$w(d_I) = \begin{cases} 1 - 6 \cdot \left(\frac{d_I}{d_{ml}}\right)^2 + 8 \cdot \left(\frac{d_I}{d_{ml}}\right)^3 - 3 \cdot \left(\frac{d_I}{d_{ml}}\right)^4 & d_I \leq d_{ml} \\ 0 & d_I > d_{ml} \end{cases}, \quad (1)$$

where $d_I = \|x - x_I\|$ is the distance between the point x and node point x_I and d_{ml} is the domain of influence of node x_I .

The general process of calculating the weight function $w_I(x)$ for node x_I and sampling point x by MCW is given by:

1. When the line (x_I, x) does not intersect any crack then point x is called *visible*. Then $w_I(x)$ is calculated by formula (1), where $d_I = \|x - x_I\|$.
2. Otherwise, the point x is *invisible* and then
 - 2.1 Look for all crack lines that are crossed by the line (x_I, x) . We call these *crossed cracks* (cracks 1, 2, 3 in Figure 1a).
 - 2.2 For all n *crossed cracks*, we look for the shortest path connecting the node point x_I with the sample point x going through one of the two tips of each of the *crossed cracks* (Figure 1a, b).

The optimal path may skip part of the *crossed cracks* tips (crack number 2 in Figure 1a) if no segment of this path crosses other *crossed cracks*. There

is a possibility that two or more cracks may have common tips. In that case, such tips cannot be included in the path (Figure 1c). We mark the tips of the *crossed* cracks that the path goes through them as $x_c^i, i=1..n$.

2.3 Modify d_I according to the selected method for modification of the weight function near the crack tip (diffraction method in this example):

$$d_I = \left(\frac{s_1 + s_2(x)}{s_0(x)} \right)^\lambda \cdot s_0(x), \quad (2)$$

where $s_0(x) = \|x - x_I\|$, λ is the diffraction parameter (for problems with equally spaced nodal distributions and a linear basis, $\lambda=2$. For the problems with a basis enrichment, λ is equal to either to 1 or 2) and $s_1, s_2(x)$ are modified according to the following rule (see Figure 2):

$$s_1 = \|x_I - x_c^{(1)}\|, \quad (3)$$

$$s_2(x) = s_2^{(1)}(x) + s_2^{(2)}(x) + \dots + s_2^{(n)}(x), \quad (4)$$

where

$$s_2^{(k)}(x) = \|x_c^{(k+1)} - x_c^{(k)}\|, \text{ for } k=1..n-1 \quad (5)$$

and

$$s_2^{(n)}(x) = \|x - x_c^{(n)}\|. \quad (6)$$

2.4 If the modified d_I satisfies $d_I \leq d_{ml}$ then the $w_I(x)$ is calculated by (1), otherwise $w_I(x)=0$.

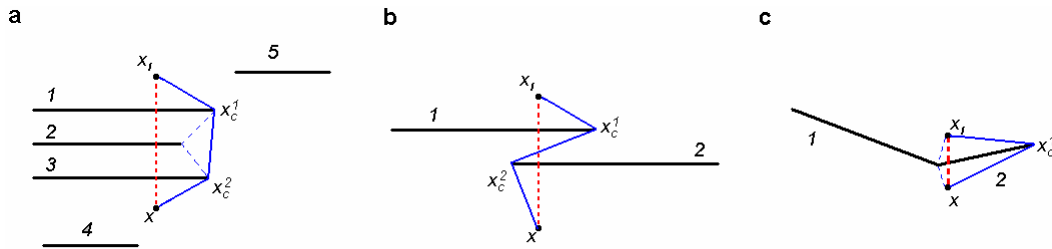


Figure 1. Paths $(x_I, x_c^{(1)}, \dots, x_c^{(n)}, x)$ for various crack configurations.

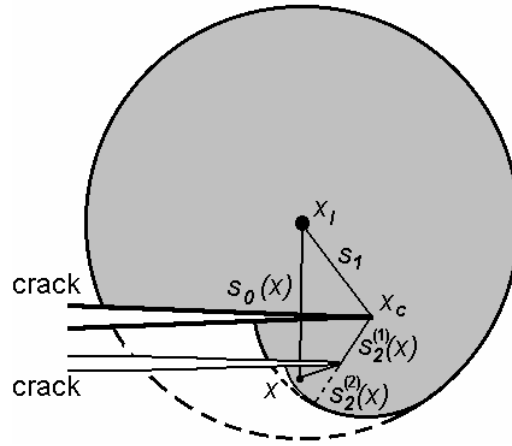


Figure 2. The weight functions modified by MCW algorithm.

In Figure 3, the weight functions for three common configurations of two cracks calculated by the diffraction method are presented.

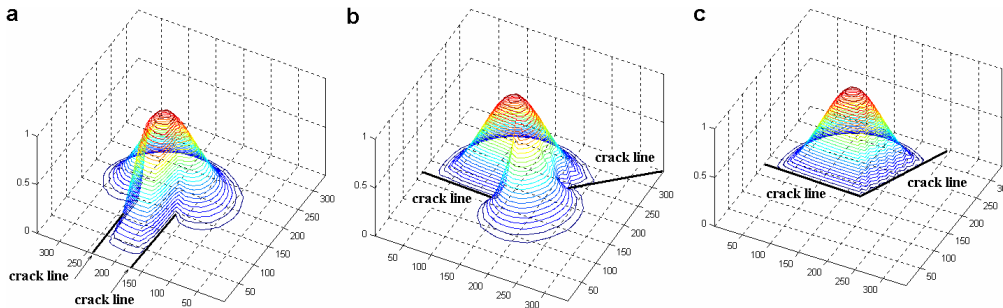


Figure 3. Spline weight functions by the diffraction method ($\lambda=2$) modified by MCW algorithm: (a) two parallel cracks, (b) two-angled and spaced cracks, (c) two-angled connected cracks.

Numerical Examples and Discussion

This section presents a study of the reliability and accuracy of the MCW method for the solution of multiple cracks problems. We consider three numerical examples of interacting and intersecting cracks. They are solved using the Element Free Galerkin (EFG) meshless numerical method [1-9]. The stress intensity factors are calculated and compared to available reference solutions provided by other numerical methods. Problems involving double-edge collinear cracks, star-shaped cracks and a system of four cracks are chosen to illustrate the main aspects of solution of multiple crack problems. These include construction of the weight functions by MCW for intersecting and interacting cracks when a number of cracks lie in the domain of influence of a single node, construction of the mesh, integration scheme, etc. The convergence of the stress intensity factors as a function of the number of nodes is analyzed and discussed.

In all the calculations the nodal distribution is equally spaced with additional nodes along the cracks surfaces and an additional node at the free tips of the cracks. In the second example of star-shaped cracks, a star-shaped array of nodes around the free tips of the cracks was used to enhance the accuracy. The radius of the outer ring of

star-shaped additional nodes was 0.75 of the distance between regular nodes. The nodal domain of influence, d_{ml} was calculated as a product of constant d_{max} and the nodal spacing parameter c_I . $d_{max}=2.5$ was used in all the calculations. This value of d_{max} was shown in [17] as optimal for various static and dynamic fracture mechanics problems. Parameter c_I is the nodal spacing, which is a distance to the second nearest node for equally spaced nodes and the distance to the third nearest node for other nodal distributions.

The above mentioned regular nodal distribution was also used as a mesh for the numerical integration using the Gauss quadrature rule with 16x16 in the first example and 12x12 Gauss quadrature points in each cell in the second and the third examples. This significant number of Gaussian points was chosen to minimize a numerical error from integration. The fully enriched basis was coupled with a linear basis at the crack tips. A plane strain condition was assumed. The MCW algorithm was used for the modification of the weight functions calculated by the spiral weight when a number of crack tips lay in the nodal domain of influence.

Double-edged collinear cracks in finite plate under normal load

To demonstrate the accuracy of the method we start with the solution of interacting double-edged collinear cracks in a finite plate, see Figure 4a. In this example we calculate the stress intensity factors for two crack geometries $a/W=0.8$ and $a/W=0.9$, and for two plate geometries $H/W=1$ and $H/W=3$. Meshes with 21x21 and 21x61 regular nodes and additional nodes around the crack tips were used for the cases $H/W=1$ and $H/W=3$, respectively. In all four cases the constructed mesh had a number of nodes with domains of influence that intersected two cracks (Figure 4c and Table 1, column N). Normalized stress intensity factors $F_I = K_I / \sigma \sqrt{\pi a}$ were calculated and compared to three available reference solutions, see Table 1.

In the first solution (Table 1 ref 1) by Bowie [21], approximate stress intensity factors were calculated by:

$$K_I = \sigma \sqrt{2W \tan \frac{\pi a}{2W} \eta \left(\frac{a}{W}, \frac{H}{W} \right)}, \quad K_{II} = 0. \quad (7)$$

The values of the function $\eta \left(\frac{a}{W}, \frac{H}{W} \right)$ are presented in Table 2.

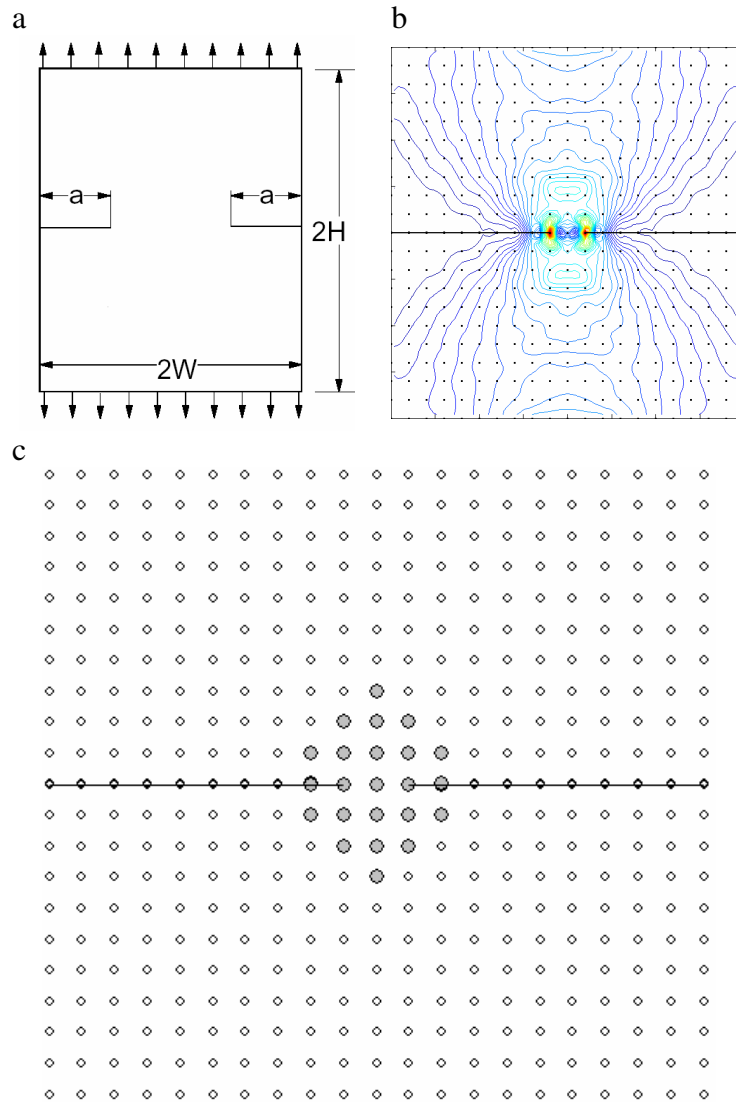


Figure 4. (a) Double-edge collinear cracks in finite plate. (b) Von Mises stress distribution for $a/W=0.9$ and $H/W=1$. (c) Nodal distribution for $a/W=0.9$ and $H/W=1$. Filled nodes represent nodes whose domains of influence intersect both cracks.

Table 1. Normalized stress intensity factors for a double-edged crack in a finite plate.

	F_I	F_I ref1	F_I ref2	F_I ref3	E_1 , %	E_2 , %	E_3 , %	N
$a/W=0.8, H/W=1$	1.6111	1.5806	1.5962	1.6432	1.93	0.93	1.96	11
$a/W=0.8, H/W=3$	1.5497	1.5649	-	-	0.97	-	-	11
$a/W=0.9, H/W=1$	2.1326	2.1133	-	-	0.91	-	-	25
$a/W=0.9, H/W=3$	2.1016	2.1133	-	-	0.55	-	-	25

$E_{1,2,3}$ represents the percent difference of normalized stress intensity factors, F_I with reference solutions F_I ref 1,2,3. We note that for the two last cases, the normalized stress intensity factors F_I ref1 were identical despite the difference in the geometry of the specimen ($H/W=1$ and $H/W=3$).

N represents number of nodes whose domain of influence crosses both cracks.

Table 2. Values of the function $\eta\left(\frac{a}{W}, \frac{H}{W}\right)$.

a/W	0.8	0.9
$H/W=1$	1.01	1.00
$H/W=3$	1.00	1.00

The accuracy of Bowie's solution is unknown. However, in the case of a semi-infinite plate the accuracy of his solution was about of 99% compared with the approximating solution of Irwin, see [22].

Two other solutions for the function $\eta\left(\frac{a}{W}, \frac{H}{W}\right)$ are provided by the method of Denda and Dong [23] for the cases $a/W=0.8$ and $H/W=1$. These values were 1.02 by the *whole crack element* and 1.05 by the *crack tip element*. Applying formula (7) the normalized stress intensity factors were 1.5962 (Table 1 ref 2) and 1.6432 (Table 1 ref 3) respectively.

The results of the numerical example show that the proposed method provides solution which in 99% agreement with the reference solutions in all four cases with relatively small nodal density. This is due to the ability to simultaneously characterize several discontinuities in a single domain of influence. It is important to note that solution of the same problem with the standard EFG method requires significantly dense nodal distribution with smaller domain of influence to avoid more than one discontinuity in a domain of influence. For example, in the case $a/W=0.9$ and $H/W=1$, one forced to use at least 71×71 nodes for solution by the regular EFG method. The new method with 21×21 regular nodes has similar accuracy to EFG with 71×71 nodes and requires a factor of 14 less computer time than EFG. The necessity of the fine meshes is dictated by limitations in the construction of the weigh functions and is not due to the ability of the method to provide an accurate solution with a smaller number of nodes.

Star-shaped crack in finite plate under bi-axial load

We next consider six intersecting cracks that were used to model a star-shaped crack (Figure 5a). The normalized stress intensity factors $F_I^A = K_I^A / \sigma\sqrt{\pi a}$, $F_I^B = K_I^B / \sigma\sqrt{\pi a}$ and $F_{II}^B = K_{II}^B / \sigma\sqrt{\pi a}$ were calculated using the domain form of the interaction integral for $a/W=0.5$ and several ratios of a/h , where a is the crack length and h is the average nodal spacing. The results presented in Figure 6 show the convergence of the solution as the mesh is refined. The stress intensity factors are oscillating while they converge to their limiting values. The amplitude of the oscillations vanishes as the ratio a/h increases. The relative differences between the stress intensity factors, F_I^A , F_I^B , F_{II}^B calculated with $a/h=5$ mesh and those calculated with $a/h=10$ were 0.23%, 0.20%, 0.75% respectively.

Comparing these results with the reference solutions [24,25], one sees that the accuracy of the solution is acceptable even for the relatively small ratio of $a/h=5$

(mesh with 21x21 regular nodes) and that the results agree satisfactorily with those in [24,25] (Table 3, case $a/W=0.5$). This is despite the fact that the small regular nodal distribution cannot match the inclined crack lines properly, several cells of the integration mesh are crossed by cracks and two crack tips are in the nodal domain of influence of many nodes (Figure 5c and Table 3 column N). This demonstrates that the EFG method combined with the spiral weight and MCW methods is able to solve accurately multiple crack problems with even relatively small nodal distributions.

Next we solve the star-shaped crack problem for different a/W ratio. For the ratio a/W equal to either 0.5, 0.6, 0.7 or 0.8, the regular mesh had 21x21 nodes. For smaller values of a/W we preserve the ratio $a/h=5$. The calculated normalized stress intensity factors (Table 3) were compared with those calculated by X-FEM in [24] for two different meshes distributions (Table 3 ref 1 and ref 2) and by Cheung et al in [25]. Our results show good agreement with the reference results and are closer to those provided by X-FEM than to results of Cheung et al.

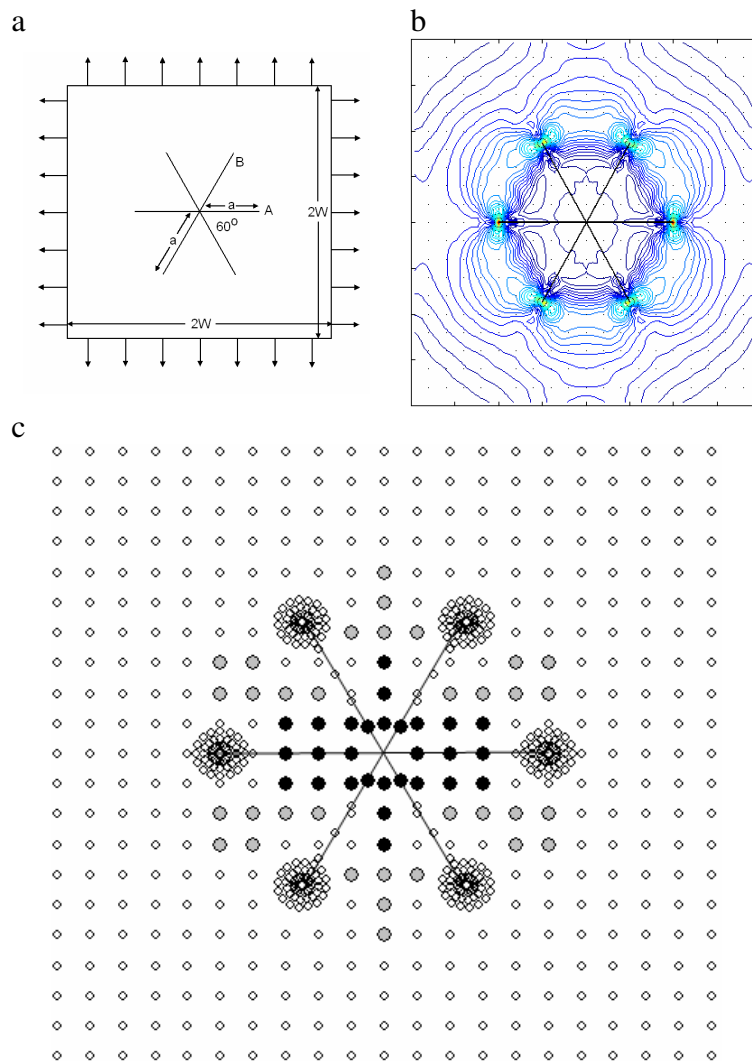


Figure 5. (a) Finite-size plate with star-shaped crack under bi-axial loading. (b) Von Mises stress distribution for $a/W=0.5$. (c) Mesh distribution for $a/W=0.5$. Filled dark and grey nodes represent nodes whose domains of influence intersect six and two cracks respectively.

Table 3. Normalized stress intensity factors for the problem in Figure 5.

		F_I	F_I ref 1	F_I ref 2	F_I ref 3	$E_1, \%$	$E_2, \%$	$E_3, \%$	N
$a/W=0.2$	F_I^B	0.7690	0.7683	-	0.7578	0.09	-	1.48	80
$a/W=0.2$	F_{II}^B	0.0007	0.0005	-	0.0004	*	-	*	80
$a/W=0.2$	F_I^A	0.7691	0.7670	0.7746	0.7570	0.27	0.71	1.60	80
$a/W=0.3$	F_I^B	0.7994	0.7983	0.7973	0.7884	0.14	0.26	1.40	50
$a/W=0.3$	F_{II}^B	0.0020	0.0021	0.0021	0.0022	*	*	*	50
$a/W=0.3$	F_I^A	0.7970	0.7931	0.7942	0.7846	0.49	0.35	1.58	50
$a/W=0.4$	F_I^B	0.8527	0.8466	0.8466	0.8365	0.72	0.72	1.94	68
$a/W=0.4$	F_{II}^B	0.0077	0.0080	0.0064	0.0070	*	*	*	68
$a/W=0.4$	F_I^A	0.8352	0.8287	0.8332	0.8255	0.78	0.24	1.18	68
$a/W=0.5$	F_I^B	0.9232	0.9255	0.9208	0.9087	0.25	0.26	1.60	72
$a/W=0.5$	F_{II}^B	0.0201	0.0184	0.0168	0.0168	*	*	*	72
$a/W=0.5$	F_I^A	0.8921	0.8864	0.8928	0.8815	0.64	0.08	1.20	72
$a/W=0.6$	F_I^B	1.0405	1.0445	1.0401	1.0182	0.38	0.04	2.19	88
$a/W=0.6$	F_{II}^B	0.0451	0.0364	0.0350	0.0388	*	*	*	88
$a/W=0.6$	F_I^A	0.9749	0.9673	0.9760	0.9758	0.79	0.11	0.09	88
$a/W=0.7$	F_I^B	1.2384	1.2367	1.2369	1.1936	0.14	0.12	3.75	88
$a/W=0.7$	F_{II}^B	0.0622	0.0593	0.0614	0.0529	*	*	*	88
$a/W=0.7$	F_I^A	1.1022	1.0971	1.1120	1.1142	0.46	0.88	1.08	88
$a/W=0.8$	F_I^B	1.5577	1.5624	1.5593	-	0.30	0.10	-	88
$a/W=0.8$	F_{II}^B	0.0804	0.0864	0.0826	-	*	*	-	88
$a/W=0.8$	F_I^A	1.3454	1.3423	1.3581	-	0.23	0.94	-	88
$a/W=0.9$	F_I^B	2.1605	2.1927	2.1659	-	1.47	0.25	-	90
$a/W=0.9$	F_{II}^B	0.0906	0.0868	0.088	-	*	*	-	90
$a/W=0.9$	F_I^A	1.9146	1.9037	1.9578	-	0.57	2.21	-	90

$E_{1,2,3}$ represents the percent difference of normalized stress intensity factors F_I^A, F_I^B with reference solutions ref 1,2,3. * Percent difference is not representative in this case since the calculated and reference values of F_{II}^B are small or close to zero. We note that in this case there is even a significant percent difference between the three reference solutions.

N represents number of nodes whose domains of influence crosses two or more cracks.

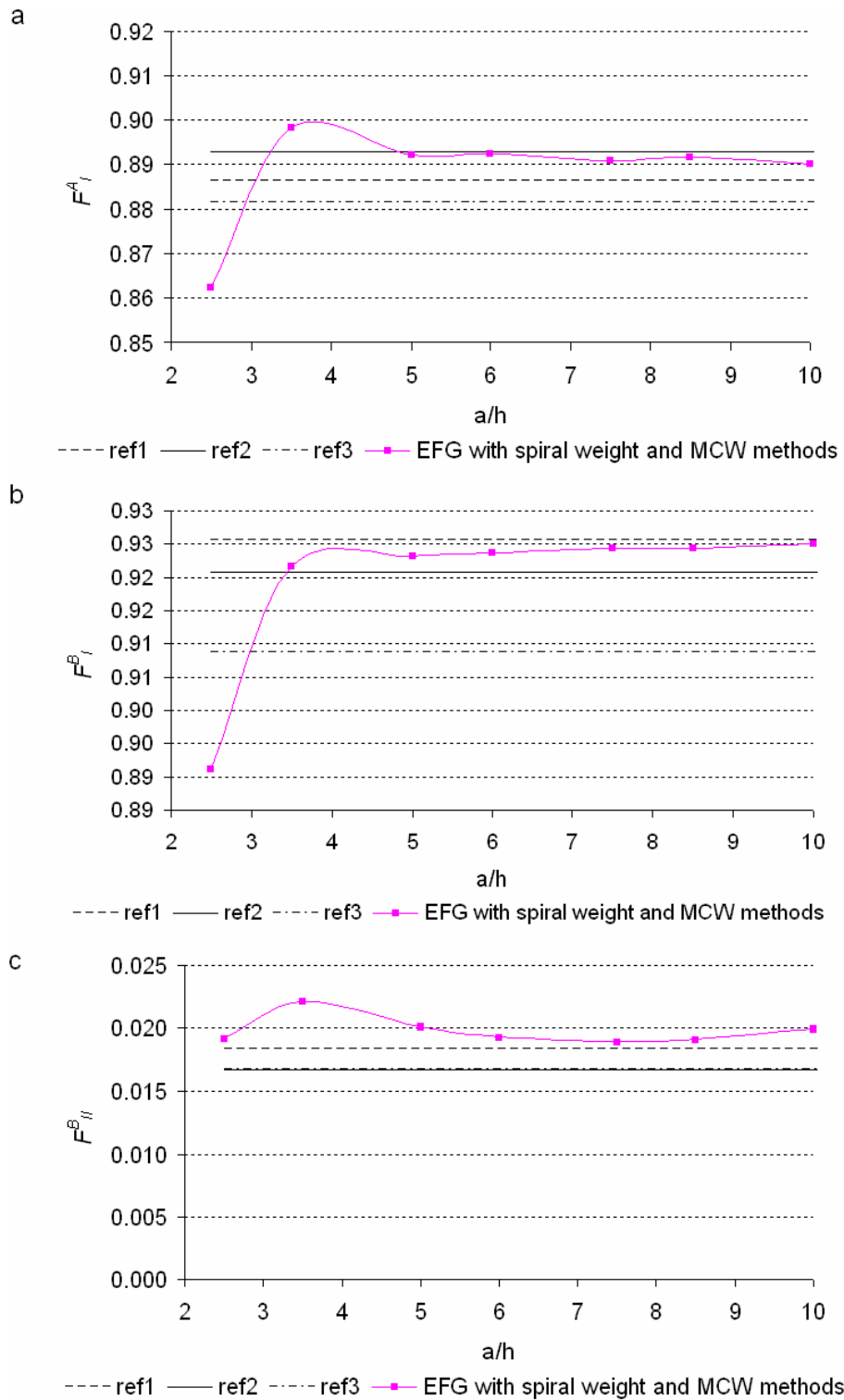


Figure 6. Convergence of the normalized stress intensity factors (a) F_I^A , (b) F_I^B , (c) F_{II}^B as a function of average nodal spacing. The results of ref 2 and ref 3 in (c) are identical.

System of four cracks in finite plate under normal load

In the next example we consider a system of four interacting cracks (Figure 7). In contrast to the previous case, these cracks are not intersecting. They positioned so that their tips are located in close proximity to each other. Such crack configuration poses

a significant challenge to numerical methods because all four adjacent crack tips are located in the stress singularity dominated area of each other. Moreover, application of different mesh refinement and enrichment techniques is limited in this case. Also a huge number of nodes (131x131 regular nodes) are required to avoid more than one crack in any nodal domain of influence and to provide enough degrees of freedom to accurately capture adjacent crack singularities. This makes implementation of the solution by regular EFG method on a personal computer almost impractical.

Nevertheless these difficulties can be minimized by MCW method. For the solution of the problem we use meshes with 41x41, 51x51, 61x61, 71x71 and 81x81 (case 1, 2, 3, 4 and 5 respectively) equally spaced nodes. In all five cases there are several nodes that have two, three or four crack tips in their domain of influence (Figure 7c, Table 4, column N). The results of calculations show that the normalized stress intensity factor $F_I = K_I / \sigma \sqrt{\pi a}$ for cases 1-4 are within 99.5% agreement with the results obtained in case 5 with the largest number of nodes (Figure 8, Table 4). Considering Von Mises stress distribution (Figure 7b) one can see strong interaction between four adjacent crack tips which are located in the stress singularity dominated area of each other. The singularities at the crack tips are accurately captured and stresses are smooth despite complex crack geometry and relatively small number of nodes. Thus, the results of the numerical example shows that the number of nodes necessary to achieve an accurate solution with MCW method is far below minimal number of nodes (131x131) required by the regular EFG method in order to avoid more than one discontinuity in nodal domain of influence.

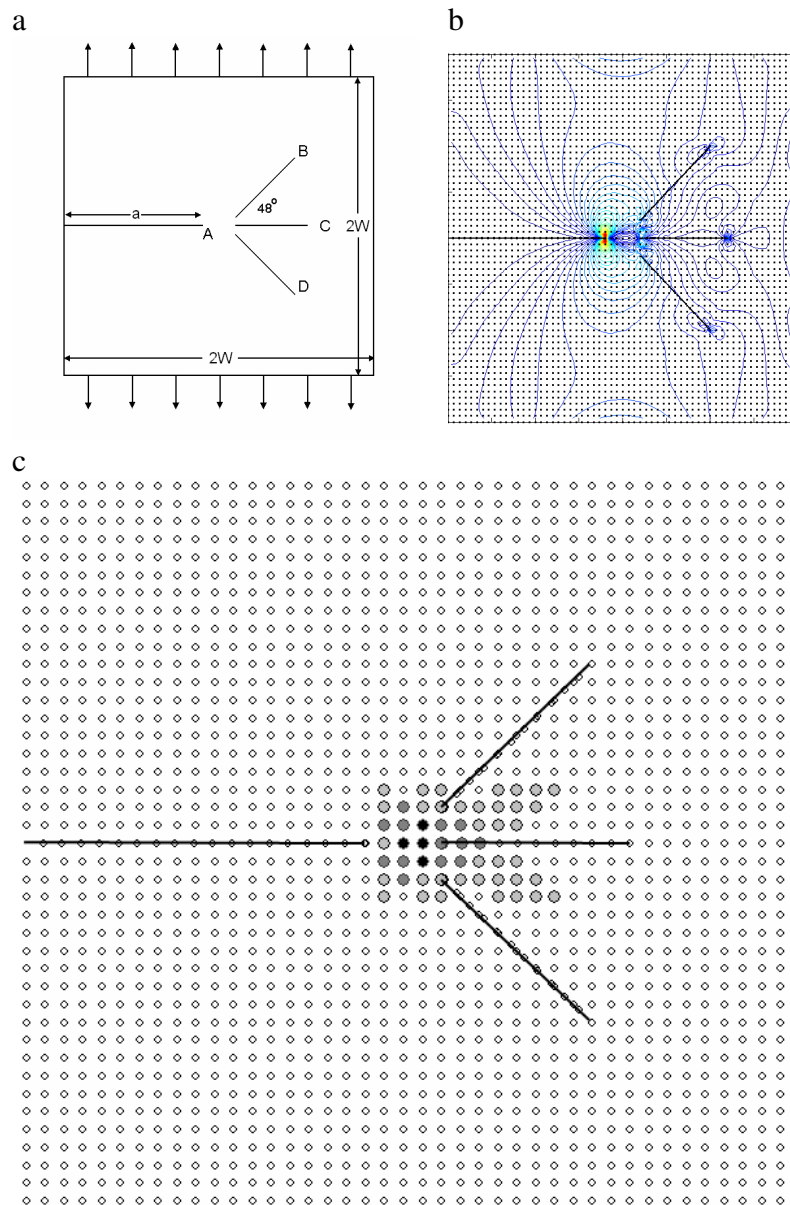


Figure 7. (a) Finite-size plate with four cracks under normal loading. (b) Von Mises stress distribution for 61x61 mesh. (c) Mesh distribution with 41x41 regular nodes. Filled black, dark grey, grey nodes represent nodes whose domains of influence intersect four, three and two cracks respectively. Defining the origin in the middle point of the specimen in (a) and W equal 2 then the coordinates of cracks A , B , C and D tips are $(0.2,0)$ - $(-2,0)$; $(0.2,0.2)$ - $(1,1)$; $(0.2,0,1.2,0)$ and $(0.2,-0.2)$ - $(-1,-1)$ respectively.

Table 4. Normalized stress intensity factors for problem in Figure 7.

Mesh	a/h	F_I	$E, \%$	N
41x41	22.22	2.787641	0.4819	59
51x51	27.78	2.813881	0.4549	50
61x61	33.33	2.810926	0.3494	46
71x71	38.89	2.801350	0.0075	39
81x81	44.44	2.801140		32

E represents the percent difference of normalized stress intensity factors F_I , with reference F_I calculated for 81x81 nodes.

N represents number of nodes those domain of influence intersect two, three or four cracks..

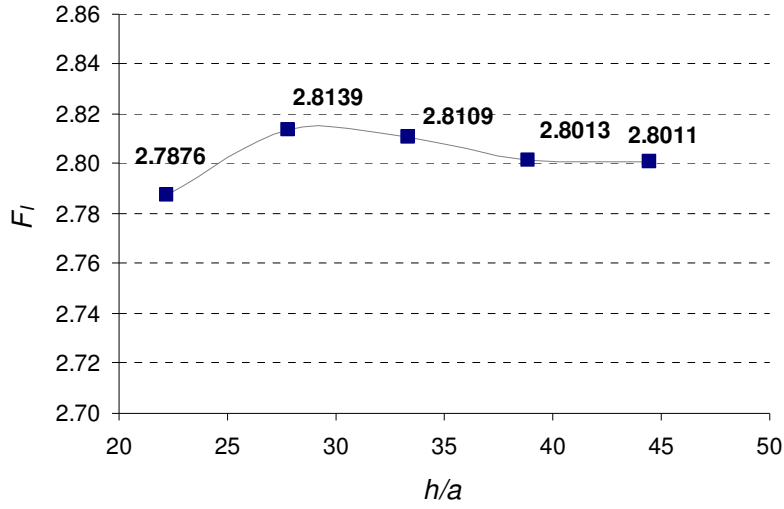


Figure 8. Convergence of the normalized stress intensity factors F_I as a function of average nodal spacing.

Conclusion

We create the multiple crack weight method for the construction of nodal weight functions around cracks. They simultaneously characterize all cracks present in the nodal domain of influence. This allows the solution of strongly interacting static and dynamic cracks without enormous mesh refinement and significantly reduces the computational efforts. In the first numerical example, the computational time for the MCW method was 14 times less compared with the EFG method. This occurred because coarser nodal distributions are required compared with the standard EFG method for comparable accuracy. The time difference is even larger when the system of many strongly interacting cracks covers a significant part of the domain.

The reliability and the accuracy of the new technique for analyzing multiple crack interactions was demonstrated by solving several problems and comparing the calculated normalized stress intensity factors with available reference solutions. The solution for the case of the double-edge collinear cracks in a finite plate reveals good agreement with three available reference solutions (Table 1). For all of the four considered cases, the solution was in 99% agreement with at least one of the references solutions for that case. Calculations for a star-shaped crack in a finite plate under bi-axial loading give good agreement compared with reference results obtained by X-FEM in [24] and by Cheung et al [25] (Table 3). There is less than a 0.5% difference between the present calculation and at least one of the three reference values for the normalized stress intensity factors F_I^A and F_I^B , in all the cases with one exception each for F_I^A and F_I^B . In the third example, the solution of a complex problem about four interacting cracks showed convergence and accurate capturing of stress singularities using EFG and MCW methods with a number of nodes which is significantly smaller than one required by regular EFG method.

References

1. Belytschko, T., Lu, Y.Y., and Gu, L., "Element-Free Galerkin Methods." *International Journal for Numerical Methods in Engineering*, Vol. 37, 1994, pp. 229-256.
2. Belytschko, T., Gu, L., Lu, Y.Y., "Fracture and Crack Growth by Element-Free Galerkin Methods" *Modeling Simulation for Materials Science and Engineering* Vol. 2, 1994, pp. 519-534.
3. Lu, Y.Y., Belytschko, T., Tabbara, M., "Element-Free Galerkin Method for Wave Propagation and Dynamic Fracture" *Computer Methods in Applied Mechanics and Engineering*, Vol. 126, 1995, pp. 131-153.
4. Belytschko, T., Lu, Y.Y., Gu, L., "Crack Propagation by Element-Free Galerkin Methods" *Engineering Fracture Mechanics* Vol. 51(2), 1995, pp. 295-315.
5. Belytschko, T., Lu, Y.Y., Gu, L., Tabbara, M., "Element-Free Galerkin Methods for Static and Dynamic Fracture" *International Journal of Solids and Structures*, Vol. 32(17-18), 1995, pp. 2547-2570.
6. Belytschko, T., Krongauz, Y., Fleming, M., Organ, D., and Liu, W.K., "Smoothing and Accelerated Computations in the Element Free Galerkin Method," *Journal of Computational and Applied Mathematics*, Vol. 74, 1996, pp. 111-126.
7. Belytschko, T., Krongauz, Y., Organ, D., Fleming, M., Krysl, P., "Meshless Methods: An Overview and Recent Developments." *Computer Methods in Applied Mechanics and Engineering*, Vol. 139, 1996, pp. 3-47.
8. Belytschko, T., Tabbara, M., "Dynamic Fracture Using Element-Free Galerkin Methods" *International Journal for Numerical Methods in Engineering*, Vol. 39, 1996, pp. 923-938.
9. Krysl, P., Belytschko, T., "Element-Free Galerkin Method for Dynamic Propagation of Arbitrary 3-D Cracks." *International Journal for Numerical Methods in Engineering*, Vol. 44, 1999, pp. 767-800.
10. Moës, N., Dolbow, J., Belytschko, T., "A Finite Element Method for Crack Growth without Remeshing" *International Journal for Numerical Methods in Engineering* Vol. 46, 1999, pp. 131-150.
11. Muravin, B., Turkel, E., "Advance Diffraction Method as a Tool for Solution of Complex Non-Convex Boundary Problems. Implementation and Practical Applications". *Lecture Notes in Computational Science and Engineering: Meshfree Methods for Partial Differential Equations*, (Griebel, M.; Schweitzer, M.A., Eds.) Vol. 26, Springer Verlag, 2002, pp. 307-317.
12. Duflot, M., "A Meshless Method with Enriched Weight Functions for Three-Dimensional Crack Propagation". *International Journal for Numerical Methods in Engineering* (submitted), 2005.
13. Rao, B.N., Rahman, S., "An Enriched Meshless Method for Non-Linear Fracture Mechanics." *International Journal for Numerical Methods in Engineering*, Vol. 59, 2004, pp. 197-223.
14. Belytschko, T., Ventura, G., Xu, J.X., "New Methods for Discontinuity and Crack Modeling in EFG." In *Meshfree Methods for Partial Differential Equations*. (Griebel, M.; Schweitzer, M.A., Eds.), Vol. 26, Springer Verlag, Berlin, 2002.

15. Krysl, P., Belytschko, T., "Element-Free Galerkin Method: Convergence of the Continuous and Discontinuous Shape Functions." *Computer Methods in Applied Mechanics and Engineering*, Vol. 148, 1997, pp. 257-277.
16. Terry, T.G., "Fatigue Crack Propagation Modeling Using the Element Free Galerkin Method." *Master's thesis*, 1994, Northwestern University.
17. Organ, D.J., Fleming, M.A., and Belytschko, T., "Continuous Meshless Approximations for Nonconvex Bodies by Diffraction and Transparency." *Computational Mechanics*, Vol. 18, 1996, pp. 225-235.
18. Hegen, D., "An Element-Free Galerkin Method for Crack Propagation in Brittle Materials." *Ph.D. thesis*, 1997, Eindhoven University of Technology.
19. Duflot, M., Nguyen-Dang, H., "A Meshless Method with Enriched Weight Functions for Fatigue Crack Growth" *International Journal for Numerical Methods in Engineering*, Vol. 59, 2004, pp. 1945-1961.
20. Muravin, B., Turkel, E., "Spiral Weight for Modeling Cracks in Meshless Numerical Methods" *Computational Mechanics*, Springer-Verlag, accepted for publication, 2005.
21. Bowie, O. L., "Rectangular Tensile Sheet with Symmetric Edge Cracks". *Journal of Applied Mechanics*, Vol. 31 (2), 1964, 208 p.
22. Cherepanov, G.P., "Mechanics of Brittle Fracture" /in Russian/, Moscow, Nauka, 1974, 640p.
23. Denda, M. and Dong, Y.F., "Complex Variable Approach to the BEM for Multiple Crack Problems". *Computer Methods in Applied Mechanics and Engineering*, Vol. 141, 1997, pp. 247-264.
24. Daux, C., Moes, N., Dolbow, J., Sukumar, N. and Belytschko, T., "Arbitrary branched and intersecting cracks with the extended finite element method." *International Journal for Numerical Methods in Engineering*, Vol. 48, 2000, pp. 1741-1760.
25. Cheung, Y., Wang, Y. and Woo, C., "A general method for multiple crack problems in a finite plate." *Computational Mechanics*, Vol. 10, 1992, pp.335-343.